NBS
PUBLICATIONS

NBSIR 82-1661

NAT'L INST. OF STAND & TECH R.I.C.
A11105 864912

CHARACTERIZATION OF A CONCENTRIC-CORE FIBER

A11101 110468

B. L. Danielson
D. L. Franzen
R. L. Gallawa
E. M. Kim
M. Young

National Bureau of Standards
U.S. Department of Commerce
Boulder, Colorado 80303

April 1982

QC
100
.U56
82-1661
1982
c. 2

NATIONAL BUREAU
OF STANDARDS
LIBRARY
MAY 25 1982

NBSIR 82-1661

CHARACTERIZATION OF A CONCENTRIC-CORE FIBER

B. L. Danielson
D. L. Franzen
R. L. Gallawa
E. M. Kim
M. Young

Electromagnetic Technology Division
National Engineering Laboratory
National Bureau of Standards
U.S. Department of Commerce
Boulder, Colorado 80303

April 1982

Sponsored by
Communications Systems Center
U.S. Army Communications R&D Command
Fort Monmouth, New Jersey 07703

U.S. DEPARTMENT OF COMMERCE, Malcolm Baldrige, Secretary

NATIONAL BUREAU OF STANDARDS, Ernest Ambler, Director

CONTENTS

		Page
1.	Introduction	1
2.	Attenuation	2
3.	Radiation Patterns	6
4.	Pulse Broadening	14
5.	Index Profile	16
6.	Optical Time Domain Reflectometer Signatures	17
7.	Capture Fraction	22
8.	References	23

CHARACTERIZATION OF A CONCENTRIC-CORE FIBER

B. L. Danielson, D. L. Franzen
R. L. Gallawa, E. M. Kim, M. Young*

National Bureau of Standards
Boulder, Colorado 80303

Several optical properties of a concentric-core fiber are examined. These include attenuation, radiation patterns, pulse broadening, index profile, backscatter signatures, and capture fraction. Experimental techniques are briefly described and the significance of the measured parameters is discussed.

Key words: attenuation; backscatter; backscatter signatures; capture fraction; concentric-core fiber; fiber optics; index profile; optical time domain reflectometer; OTDR; pulse broadening; radiation patterns.

1. Introduction

In partial fulfillment of obligations under the contract entitled "Optical Fiber Backscatter Studies," the Optical Electronic Metrology group at NBS has undertaken a limited number of measurements directed toward characterizing the optical properties of a concentric-core fiber provided by the U.S. Army Communications R&D Command. The current work is concerned with attenuation, radiation patterns, pulse broadening, index profile, backscatter signatures, and capture fractions. Measurements on some other important parameters, in particular crosstalk between cores, were not attempted for this report.

The concentric-core fiber contains two optical channels, in a cylindrically symmetric configuration, within a single optical fiber [1,2]. Each channel is optically isolated from the other. This geometry presents some unique measurement problems, as the cores must be excited individually. The measurement techniques and apparatus, as well as the special adaptations necessary for this unique fiber, are described in detail in the text.

The fiber used in the present work was manufactured by ITT with the designation EC20366, Cable #091178-A. The original length was 810 m, and a few meters were removed for some of the measurements.

---

*Electromagnetic Technology Division, National Engineering Laboratory.

2. Attenuation

In any electromagnetic waveguide, the attenuation of a mode is a function of mode number. Thus, the characterization of a multimode telecommunication fiber is complicated, because modal excitation efficiency is a function of launch conditions. Different laboratories, using different launch conditions, will therefore report different values of measured attenuation for the same fiber, unless steps are taken to avoid the vagaries inherent to a multimode fiber [3]. There are currently two ways of restricting launched optical power to avoid exciting certain high-loss modes (which are the source of capricious results): the beam optics, or limited phase space technique [4,5], and the mode filter approach [6,7,8]. In the beam optics technique, which is the one used here, the launch spot size and the launch numerical aperture are smaller than the fiber core and the fiber numerical aperture, respectively. The Electronics Industry Association (EIA) recommends a spot diameter that is 70 ± 5 percent of the fiber core diameter and a launch numerical aperture that is 70 ± 5 percent of the fiber numerical aperture. Figure 2-1 shows the arrangement used to limit spot size and launch numerical aperture independently.

The desired wavelength is obtained via the interference filter. Aperture A_1, is called the source aperture, and its size is changed to yield a desired launch spot size. The launch spot size is given by A_1 L'/L, where L' is the distance from A_1 to L_3 and L is the distance from L_3 to the fiber end.

The launch numerical aperture is adjusted by changing the aperture A_2.

The mode filter approach to attenuation measurements is based on an entirely different concept. While the beam optics technique attempts to launch only the desired modes, the mode filter technique calls for overfilling the fiber and then stripping off the unwanted high-loss modes. The mode filter is deemed adequate if the far-field radiation pattern is slightly more narrow than that out of a long length of the same fiber. Mode filters are specified by the amount they restrict the far-field pattern out of a short length of reference fiber. Commonly used mode filters include dummy fibers and macroscopic-bend mandrel wraps [7,8].

Tests have been conducted to determine the differences in measured values when using the two techniques [9]. There was no significant difference in the results.

The basic purpose of the two standard launch conditions is to enhance repeatability, thereby allowing a prediction of total attenuation when sections of fiber are joined (concatenation). The restricted launch conditions are adequate for this

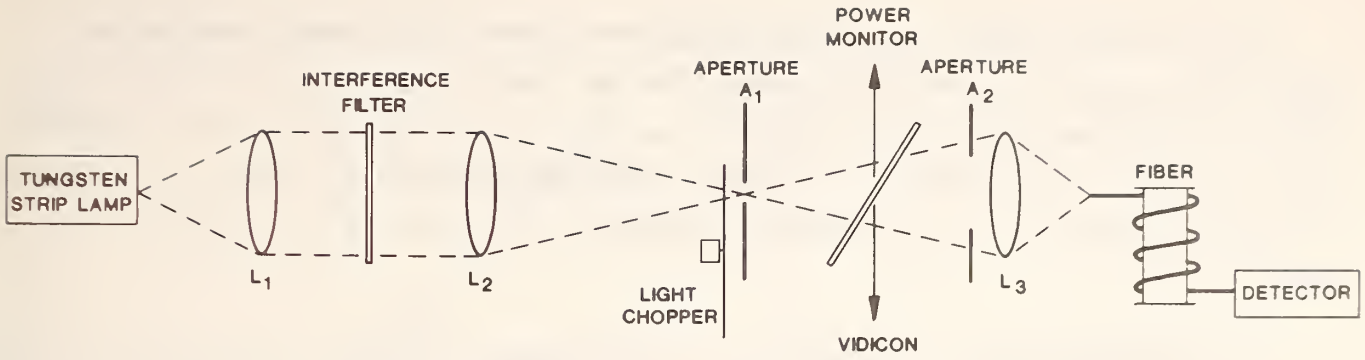

Figure 2-1. Experimental layout for attenuation measurements.

purpose. The concentric core fiber represents an interesting challenge in this regard because of its geometry. If the basis of the restricted launch concept is applied to outer core, we would seek to launch power uniformly in that outer core. This is clearly impractical. In the spirit of the limited phase space launch, the launch spot size and launch numerical aperture (LNA) were adjusted as though the width of the outer core was a diameter. Thus, the launch spot size used for the outer core was about 57 percent of 15 μm, or 8.5 μm. For the inner core, launch spot size was 21.3 μm or about 71 percent of the core size. In both cases, LNA was 0.18 or about 72 percent of the fiber NA, as reported in another part of this document.

Measured values of attenuation are given in table 1.

In measuring the attenuation of the outer core, no attempt was made to determine how measured values change with azimuthal orientation of the fiber. Power was launched into the same general area of the outer core each time the measurement was performed. We expect considerable variability in that measurement because the 8.5 μm launch spot represents only about 6 percent of the outer core area. Thus, the measured value depends critically on conditions over that 6 percent of the outer core. The precision given in the table is for the measurements performed, i.e., launch into the same part of the outer core each time.

Table 1. Measured Attenuation Cut-Back Technique

Component	Launch spot size (μm)	LNA	Attenuation (dB/km)
Inner core	21	0.18	4.81 ± 0.1
Outer core	85	0.18	4.65 ± 0.1
Outer core	21	0.18	4.77 ± 0.1

Note from the table that the oversize launch spot on the outer core yields attenuation about 0.2 dB/km greater than for the smaller launch spot. This is consistent with expectations, since overfill excites the high-loss modes that were discussed earlier. Those modes contribute to measured attenuation, with the result that values are skewed and do not reflect a reasonable value for use in predicting concatenation results.

The attenuation was also estimated by backscatter techniques as described in section 6. The OTDR and cutback comparisons are listed in table 2. It is clear that launch and other measurement procedures have an important influence on the resulting attenuation values.

We have also plotted the spectral loss according to a method proposed by Inada [10] in which attenuation is plotted as a function of the reciprocal of the fourth power of the wavelength. This type of display is particularly convenient since it allows for the ready decomposition of attenuation into Rayleigh and non-Rayleigh type component losses. If α_T represents the total loss, then

$$\alpha_T = \frac{D}{\lambda^4} + E + C(\lambda), \qquad (2\text{-}1)$$

where D is the Rayleigh scattering coefficient in units of $m^{-1}\ \mu m^4$, E is the loss contribution which is independent of wavelength, and $C(\lambda)$ is the wavelength dependent contribution (such as OH absorption) which is small in the present instance. The plots, indicated in figures 2-2 and 2-3, show that Rayleigh scattering dominates the loss in this fiber and that there is little difference in the characteristics of the inner and outer cores.

Table 2. Attenuation comparisons for a concentric-core fiber at 850 nm.

Test Method	Attenuation (dB/km) Center core	Outer core
1. Nominal (butt alignment)	4.4	5.4
2. Cutback	4.81 ± 0.1	4.77 ± 0.1
3. OTDR (max. scatter)	5.55 ± 0.04	4.98 ± 0.04
4. OTDR (max. power)	5.33 ± 0.01	4.98 ± 0.06
5. OTDR (restricted launch)	4.85 ± 0.01	4.46 ± 0.02

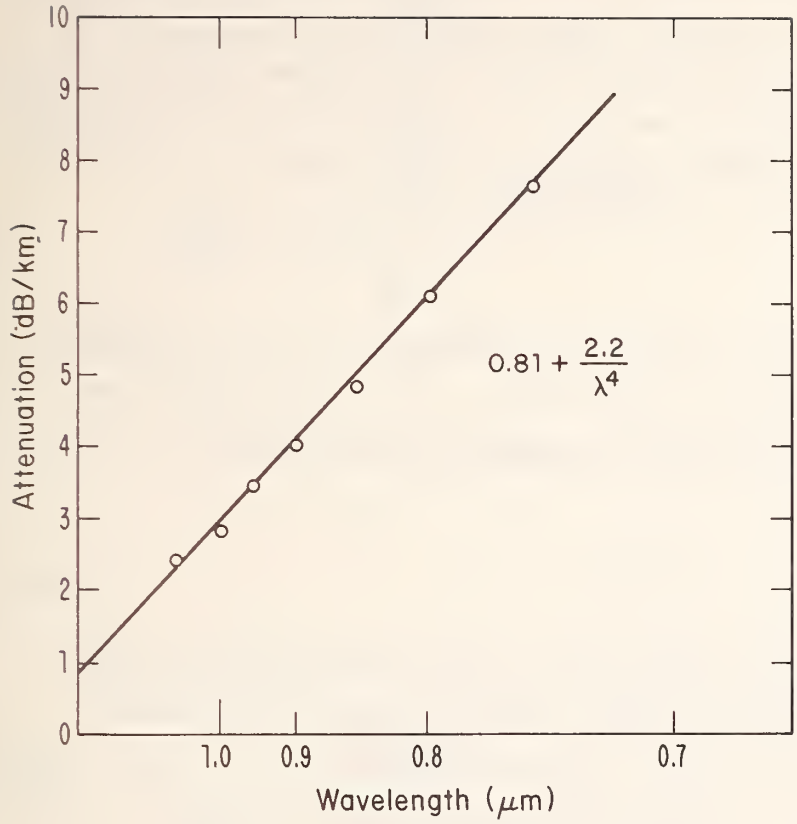

Figure 2-2. Measured loss spectra, inner core.

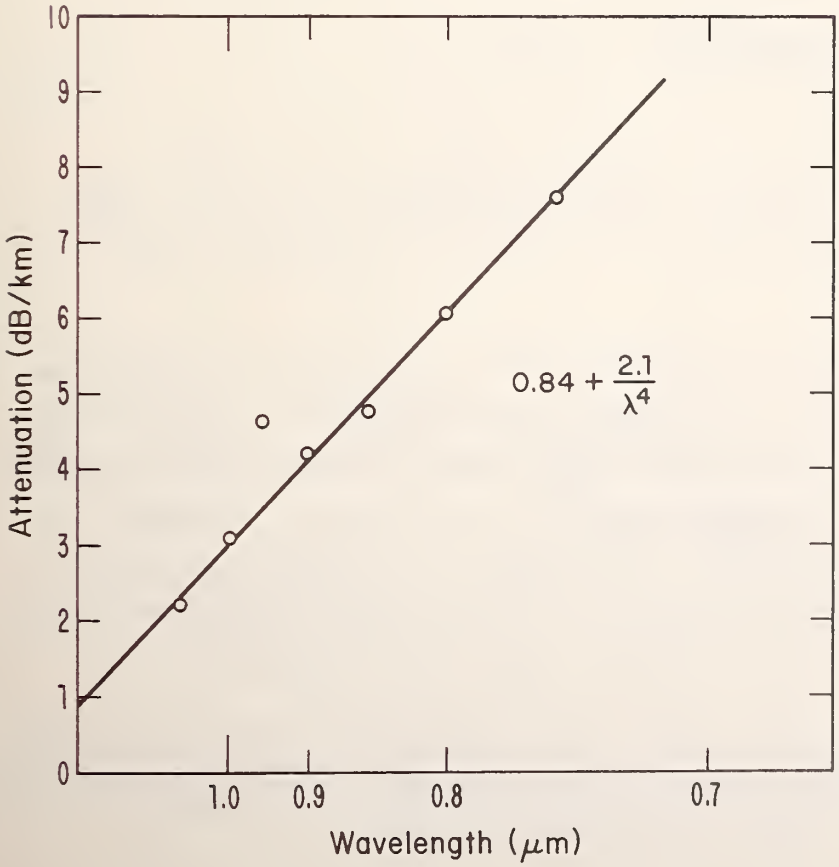

Figure 2-3. Measured loss spectra, outer core.

In the foregoing attenuation measurements we have not considered the possibility of crosstalk, which is the transfer of optical energy from one of the cores to the other. The manufacturer has specified crosstalk values in the present fiber at -22 dB inner-to-outer cores, and -26 dB outer-to-inner cores. At these levels we can safely ignore crosstalk effects in the measurements described in this report.

3. Radiation Patterns

Analyzing the radiation exiting the optical fiber can yield useful information about the fiber. The analysis may be done in the near- or far-field region of the exit end. A far-field measurement determines the angular dependence of the irradiance at a distance

$$Z_0 \geq \frac{(2a)^2}{\lambda} \tag{3-1}$$

from the fiber exit end, where λ is the wavelength of light and a the core radius. This distance is synonymous with the Fraunhofer diffraction region. The angular dependence of the exit irradiance defines the "numerical aperture (NA)" of the fiber,

$$NA = \text{Sin } \theta_0 = \sqrt{N_1^2 - N_2^2} \tag{3-2}$$

$$= N_1 \sqrt{2\Delta} \text{ with } \Delta \approx \frac{N_1 - N_2}{N_1}, \tag{3-3}$$

where N_1 is the core index of refraction, N_2 the cladding index, θ_0 the half angle where the far-field intensity has decreased to 5 percent of the maximum, and Δ is defined by the above equation.

A near-field measurement yields the spatial intensity distribution in the plane of the exit face of the fiber. Such a measurement approximates the refractive index profile of the fiber. Deviation from the true index profile results from the presence of tunneling leaky rays. Near-field measurements may also be used to determine the core diameter and ellipticity of the fiber. Leaky modes do not affect the measured width of the near-field pattern near the baseline. A core diameter measurement based on the full width at the 2 to 3 percent intensity points may be appropriate.

The radiation source for both measurements has independently variable spot sizes and NA (fig. 3-1). Aperture 1, which controls the launch spot size, is illuminated by

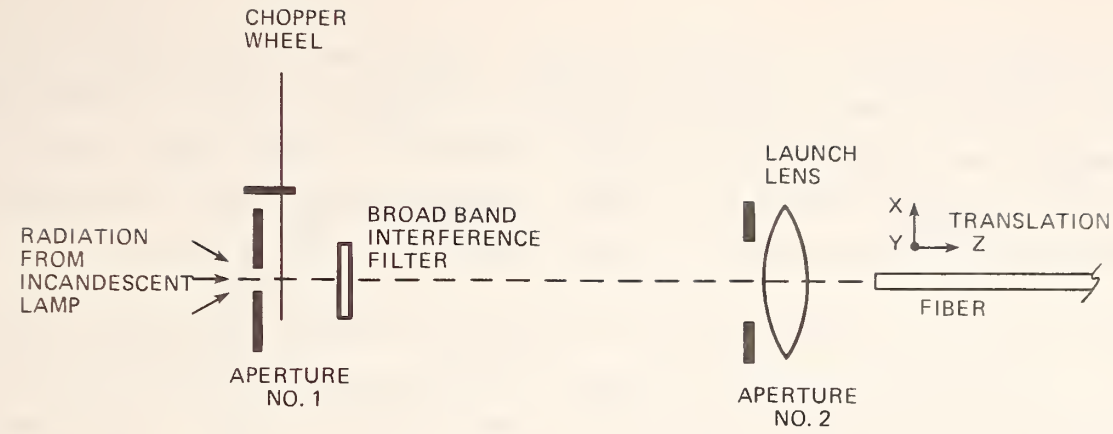

Figure 3-1. Launch optics used with far- and near-field systems.

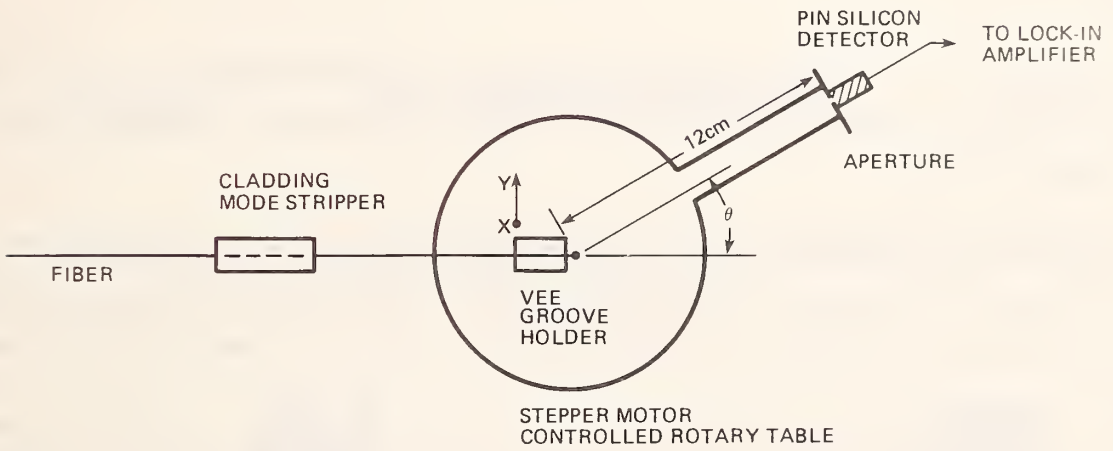

Figure 3-2. Far-field measurement system using a fixed fiber end and a rotating detector.

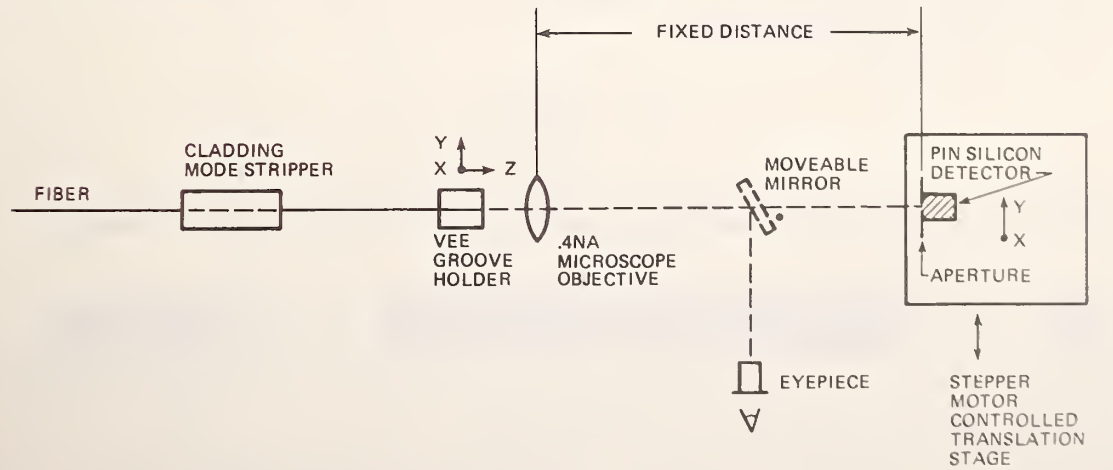

Figure 3-3. Near-field measurement system based on a radial scan of a magnified near-field image.

a quartz halogen lamp with an etched envelope. A broadband filter of 857 ± 43.5 nm was used. The launch lens produces a demagnified image of aperture 1 on the fiber end; a demagnification ratio of 22 was used. Aperture 2 controls the launch NA from a maximum of 0.36 to a minimum of 0.03. When a single core of the concentric-core fiber was illuminated the spot size of the source on the fiber was 18 μm.

The far-field was scanned using the fixed-fiber end-rotating detector method (fig. 3-2). The fiber first passes through a cladding mode stripper consisting of two 10-cm-long pieces of felt pads wetted with index matching fluids. This strips the light out of the cladding.

A vee-groove holds the fiber in place while the Si PIN detector is rotated in the far field.

Accuracy of the far-field measurement system in determining the radiation-angle measurement system is estimated to be better than 1.6 percent. The system has a dynamic range of 22 dB.

The near-field system is shown in figure 3-3. A single microscope objective produces a 50X magnified image of the fiber end face. (The near-field intensity distribution is obtained by scanning a Si PIN photodiode across a diameter of the image.)

The near-field system precision of 1.5 percent would apply to a core diameter measurement based on the near-field full width close to the baseline on a short length of fiber.

The resolution is approximately 2 μm, consistent with the calculated resolution Y, of a microscope objective with

$$Y \sim \frac{0.6\lambda}{NA}, \qquad (3\text{-}4)$$

where the NA is the collected numerical aperture (an NA of 0.2 is assumed).

The dynamic range of the near-field system is approximately 22 dB.

Measurements made with the near-and far-field systems are given in figures 3-4 to 3-12. Note the leaky mode "ears" in figure 3-4.

Further information regarding the measurement systems may be obtained from reference 11.

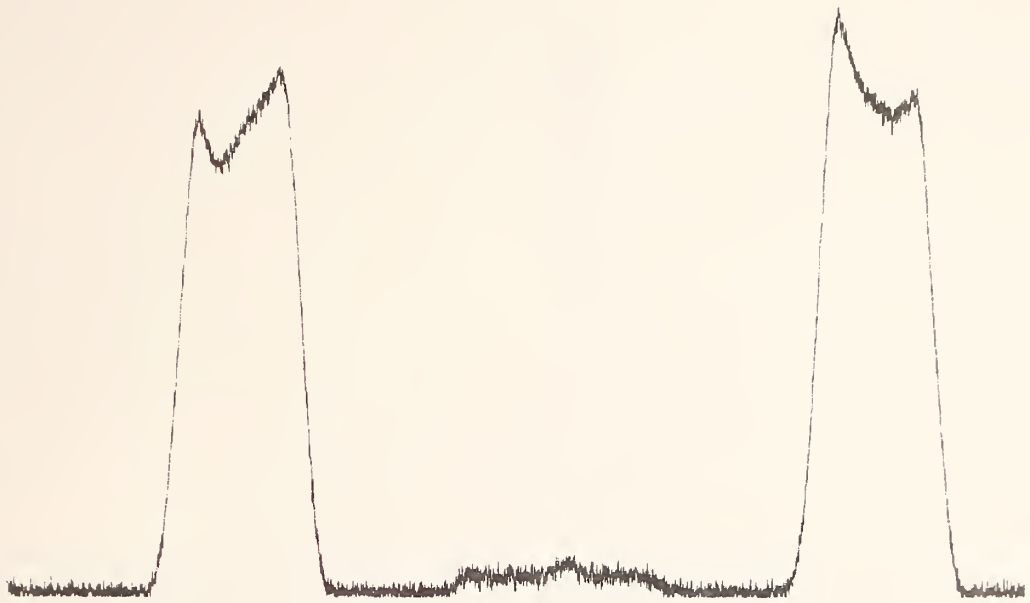

Figure 3-4. Near-field scan, 2.0 m length. Outer core excited. Leaky modes are evident.

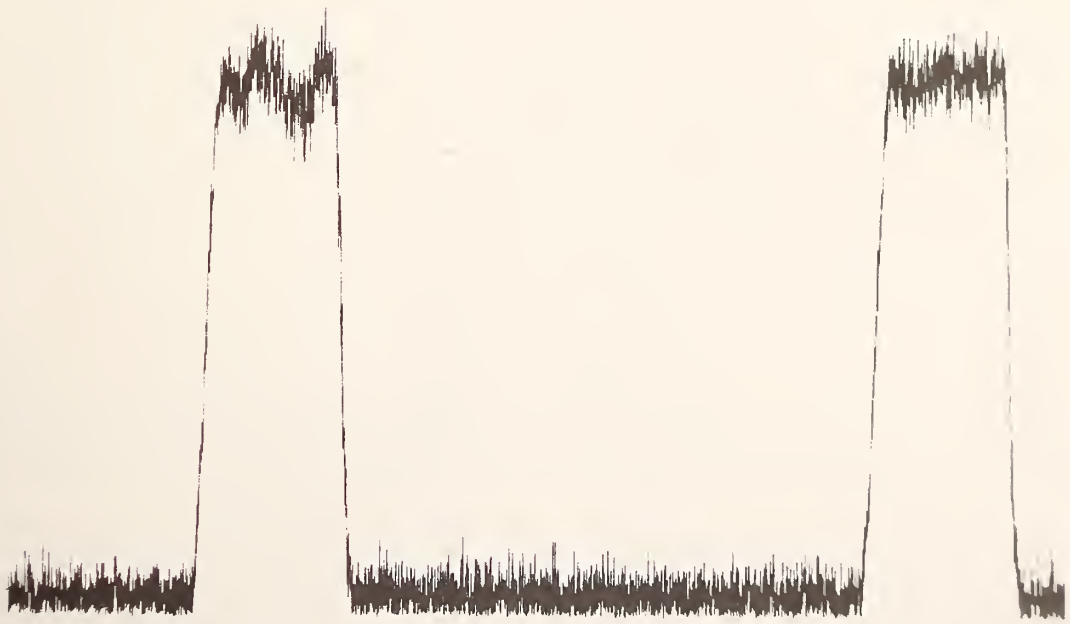

Figure 3-5. Near-field scan, 808 m length. Outer core excited. From the calibration of the scan we estimate the o.d. of the outer core at 106 μm and the corresponding i.d. at 67 μm. The crosstalk is too small to be observed on this scale.

Figure 3-6. Far-field scan, 808 m, center core excited. From the calibration we infer a numerical aperture of 0.14.

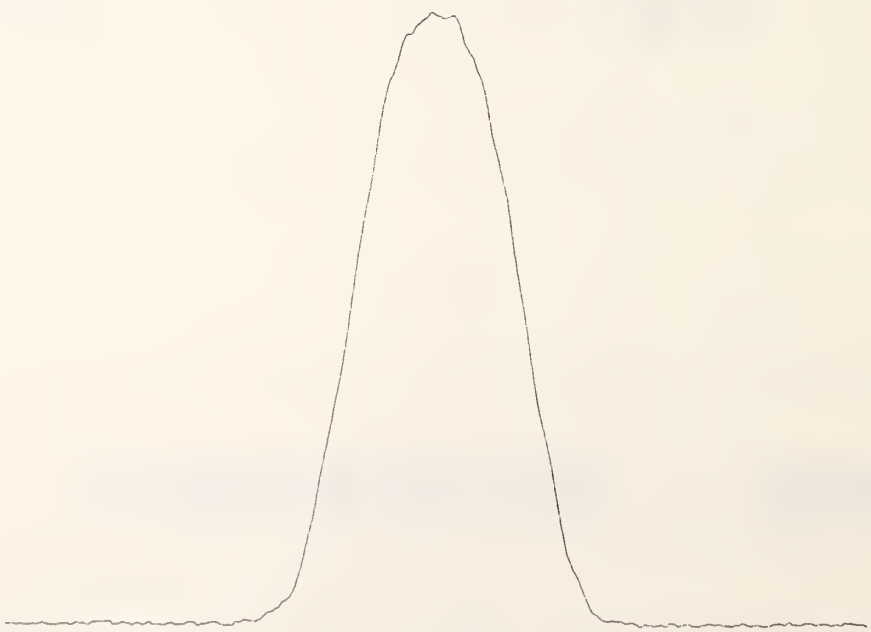

Figure 3-7. Far-field scan, 2.0 m, outer core excited.

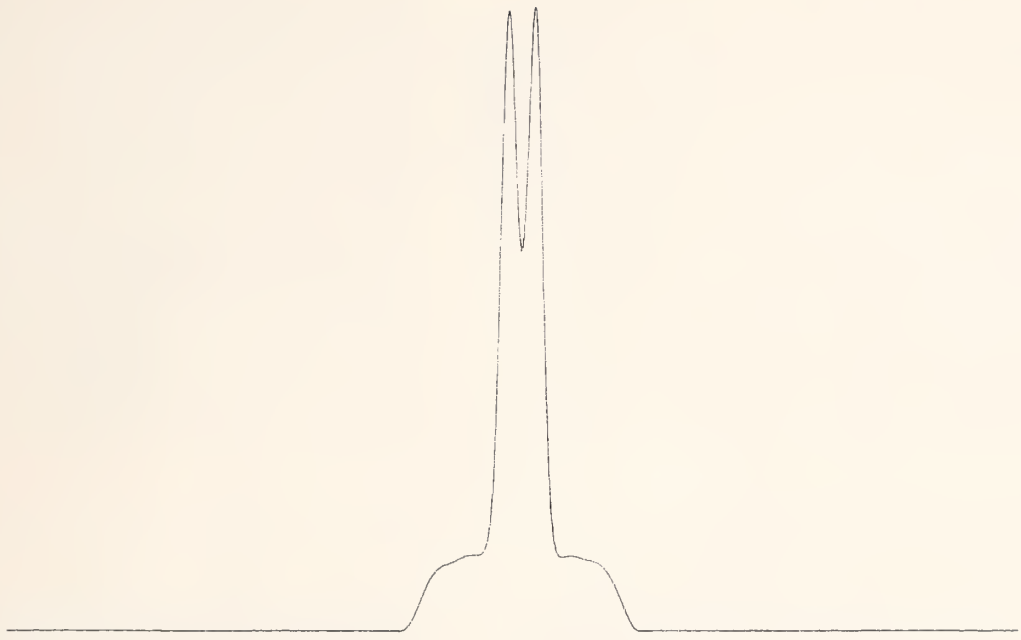

Figure 3-8. Near-field scan, 2.0 m, center core excited. Leaky modes are evident.

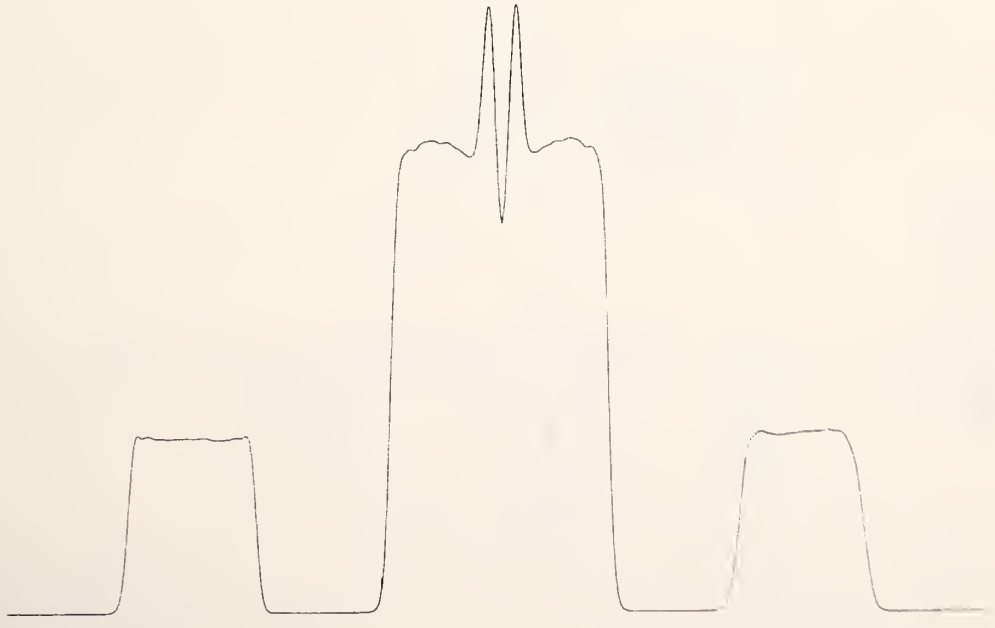

Figure 3-9. Near-field scan, 808 m, overfill launch conditions (about 55 μm input spot size).

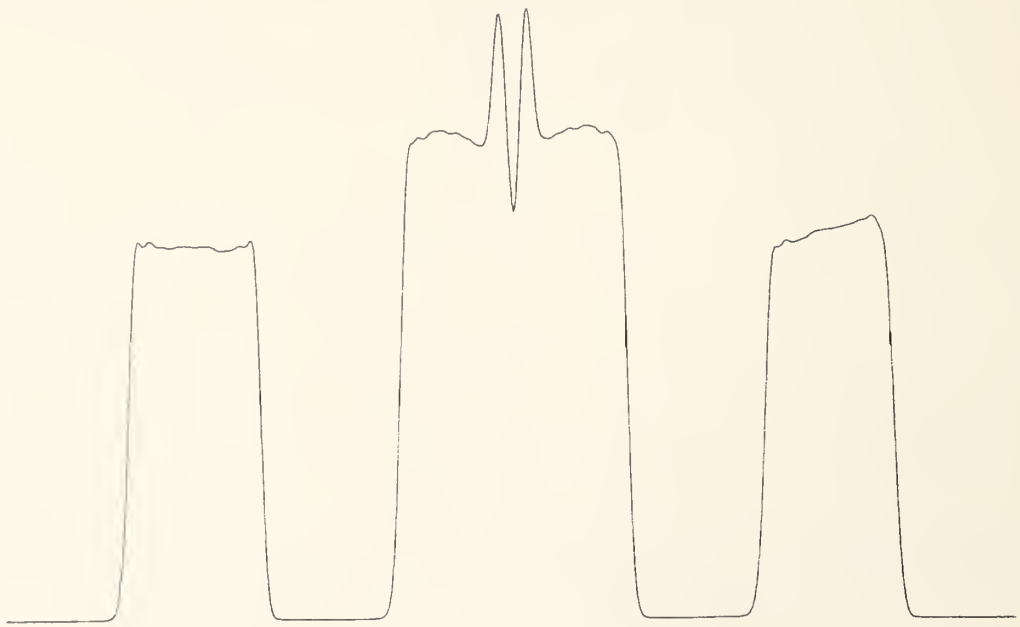

Figure 3-10. Launch conditions similar to figure 3-9, except for a 375 μm spot size.

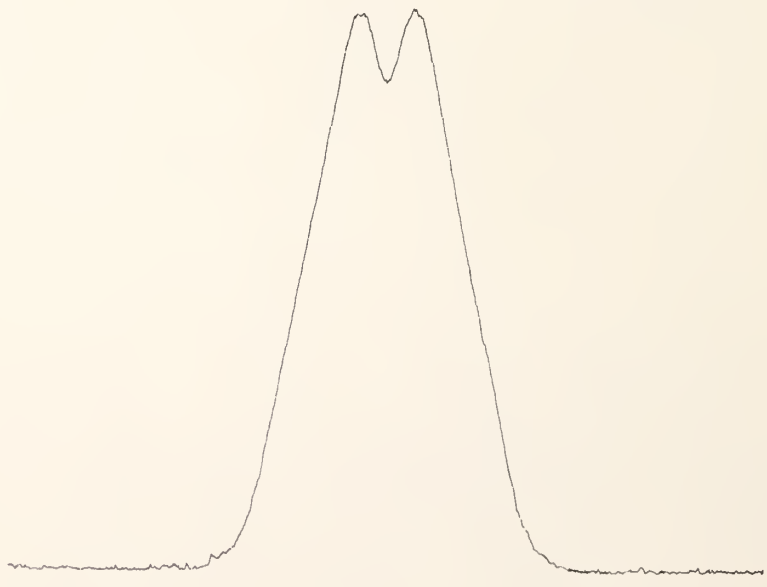

Figure 3-11. Far-field scan, 2.0 m, center core excited. The dip in this type of display is unusual.

Figure 3-12. Far-field scan, 808 m, both cores excited. From the scan calibration we measure a numerical aperture of 0.25.

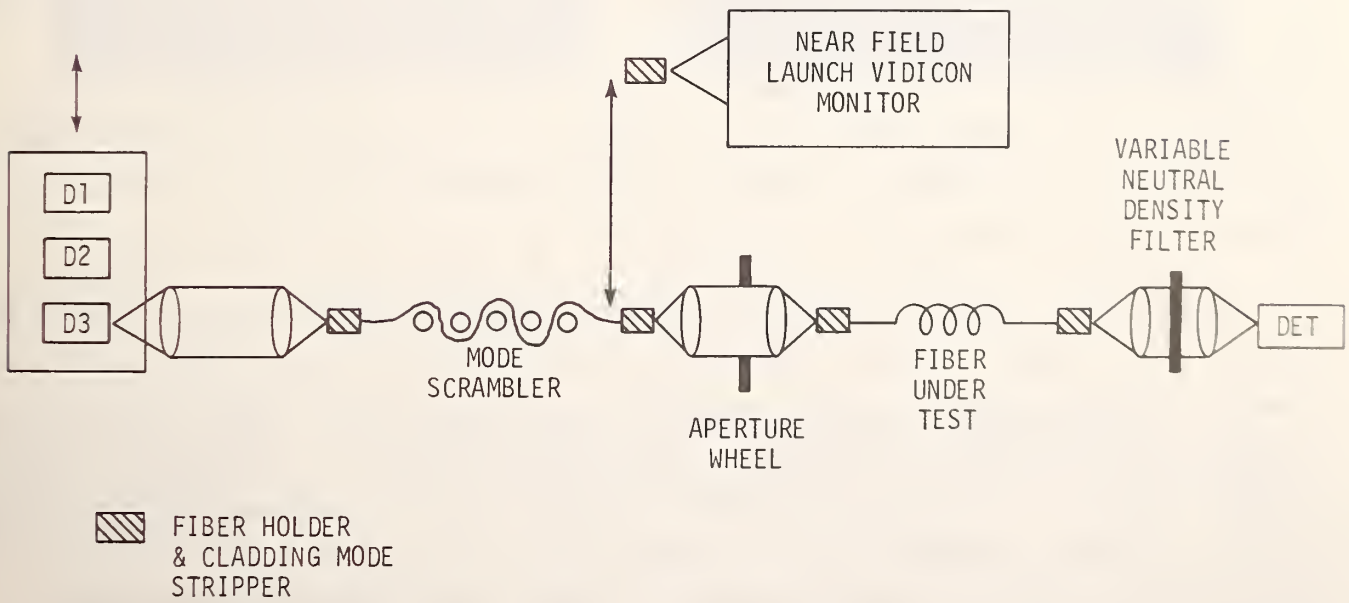

Figure 4-1. Apparatus for pulse broadening measurements.

4. Pulse Broadening

Pulse broadening, or bandwidth, is the important quantity used in determining the information carrying capacity of fibers. For a step-index fiber, the time delay between an axial ray and a ray at the critical angle is

$$\frac{L}{C}\frac{N_1}{N_2}(N_1 - N_2), \tag{4-1}$$

where L is the fiber length, C the velocity of light, N_1 and N_2 the refractive indices of the core and cladding respectively. This equation can also be expressed in terms of the fiber NA as

$$\frac{L\,(NA)^2}{2N_1C}. \tag{4-2}$$

Thus, for an NA of 0.14 the pulse broadening would be approximately 22 ns/km.

Pulse broadening measurements were made on the concentric-core fiber using the apparatus of figure 4-1. A translation stage allows one of three laser diodes to be aligned in the system. These diodes are single, heterojunction, GaAlAs laser diodes operated at 1 kHz in the short pulse mode. Pulse width is typically 300 ps full width half maximum (FWHM) and peak power launched into a fiber is in the 100-300 mW range. Figure 4-2(a) is a typical pulse shape representing the input to the fiber under test. Light from the laser diode is launched into a mode scrambler fiber consisting of a step index fiber with macroscopic serpentine bends. The mode scrambler converts the spatial radiation pattern from the diode into a unform spot which can be relaunched into the fiber under test. For the concentric core measurements, the launched spot was approximately 25 μm and could preferentially excite either inner or outer core. For more details on the bandwidth measurement system, the reader is referred to NBS Technical Note 1019 [12].

Output pulse shapes from the 810 m length concentric core fiber at a wavelength of 825 μm are shown in figures 4-2(b) and 4-2(c) (inner core) and figure 4-2(d) (outer core). The output pulse from the inner core has an approximate FWHM of 25 ns with a considerable amount of fine structure. This fine structure is a sequence of spikes (figure 4-2(c) is on expanded time base) with approximately 25-30 partially resolved pulses. We have measured a similar response from a step index fiber on only one other occasion. One possible explanation is based on the index profile, figure 5-1. The near-field scans indicate that the refractive index fluctuates near the on-axis dip. It is possible that this effect could produce another waveguide within the nominal core, and then figures 4-2(b) and 4-2(c) would indicate the differential delay of

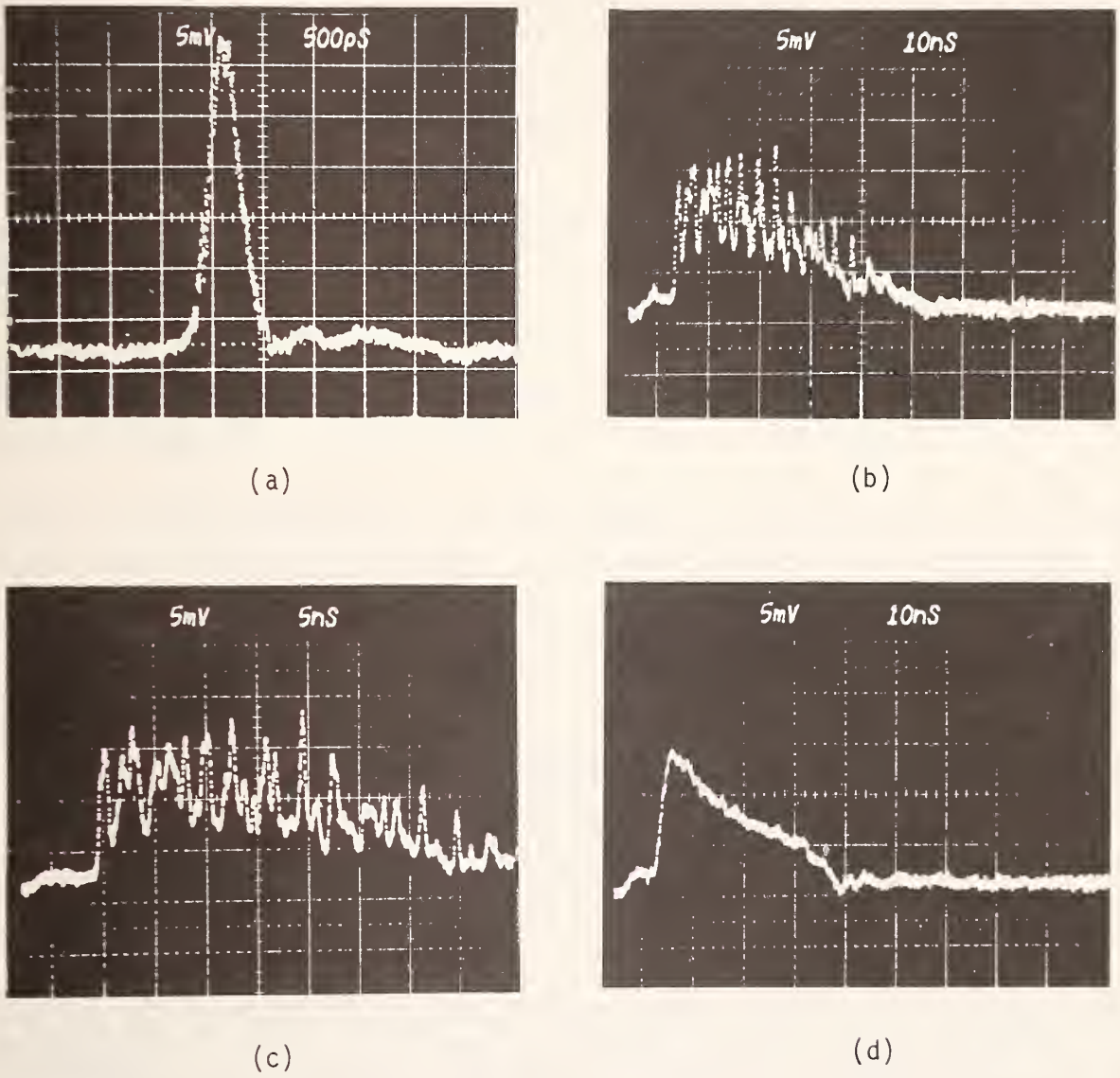

Figure 4-2. Pulse shapes for (a) input pulse; (b) and (c) inner core after 810 m; and (d) outer core after 810 m.

modes excited within this substructure. Differential delay between modes can be rather large for a fiber waveguide which has a small core and supports only a small number of modes.

The output pulse from the outer core is rather smooth in shape with a FWHM of approximately 16 ns. It should be pointed out that the near-field scans of the outer core indicate a smooth index profile over this core.

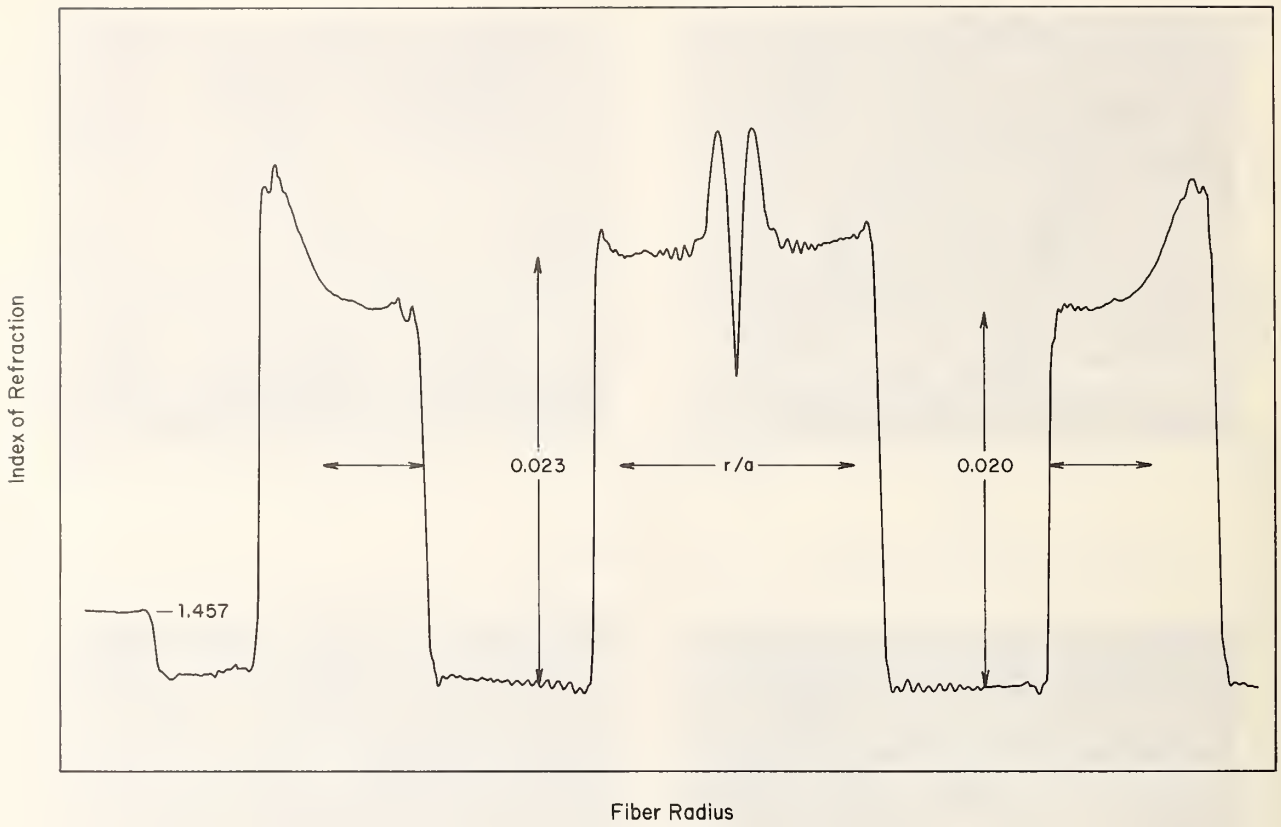

Figure 4-3. Index profile of the concentric-core fiber.

5. Index Profile

We measured the refractive index profile using the refracted ray or refracted near-field method [13,14]. To implement this technique, we focus a high numerical aperture beam onto the entrance face of the fiber. Because the NA of this beam substantially exceeds that of the fiber, a hollow cone of light is refracted (rather than reflected) at the core-cladding boundary. The innermost rays of this cone are blocked by an opaque circular stop and the rays that pass the stop are focused by high-aperture condensing optics onto a detector. The beam is scanned across the entrance face of the fiber. In most cases, the power incident on the detector is an almost precisely linear function of the refractive index of the fiber at the point where the beam is focused. We may therefore calibrate the system and thereby measure the refractive index as a function of position in the fiber entrance face.

Our system has been documented and described in detail in references 15 and 16; relative index measurements (such as core-cladding index difference) are precise to about 3 percent. The refracted ray method may also be used to measure core diameter

Table 3.

	Index difference	Numerical aperture	r/a
Inner core	0.023	0.26	0.83*
Outer core	0.020	0.24	0.86*

*Estimates.

precisely, but at the time this measurement was made we were not set up to calibrate the horizontal axis.

Figure 4-3 shows the result of a measurement of the index profile of the concentric core fiber. The ears that appear at the outer edges of both core regions are artifacts that result from the presence of leaky rays; they cannot be completely eliminated from scans of step fibers except at the expense of destroying the spatial resolution of the system.

The column in table 3 labeled r/a contains estimates of the fraction r/a of the core radius that is free of the artifacts; these estimates agree well with the appearance of the artifacts in the figure, as indicated by the horizontal arrows. (The value of r/a for the outer core region was estimated by assuming the same value as that for an ordinary step fiber the same radius as the outer cores).

Despite the artifacts, we see clearly that the indices of the two core regions are not identical. The numerical apertures of the two core regions also have been calculated from the index data and are shown in table 3.

Figure 4-3 also shows a central index depression surrounded by an annulus with higher index than that of the core as a whole; this structure is real and not an artifact of the measurement process. Likewise, most of the oscillations (except some of those right at the core-cladding boundaries) are real index fluctuations that result from the manufacturing method.

6. Optical Time Domain Reflectometer Signatures

The backscatter signatures presented in this section have been generated with the optical time domain reflectometer (OTDR) described in detail in reference 17. A block diagram of the apparatus is shown in figure 6-1. The measurements were made at a

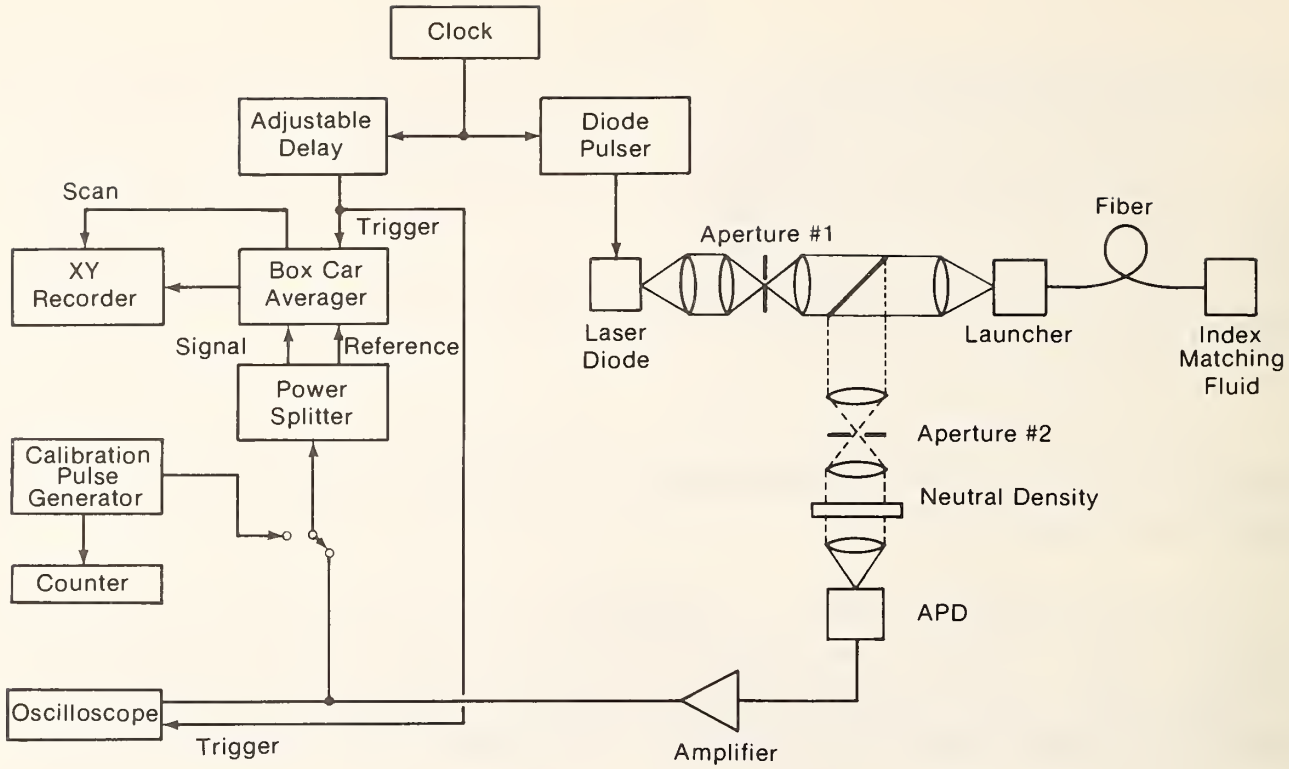

Figure 6-1. Block diagram of the OTDR system.

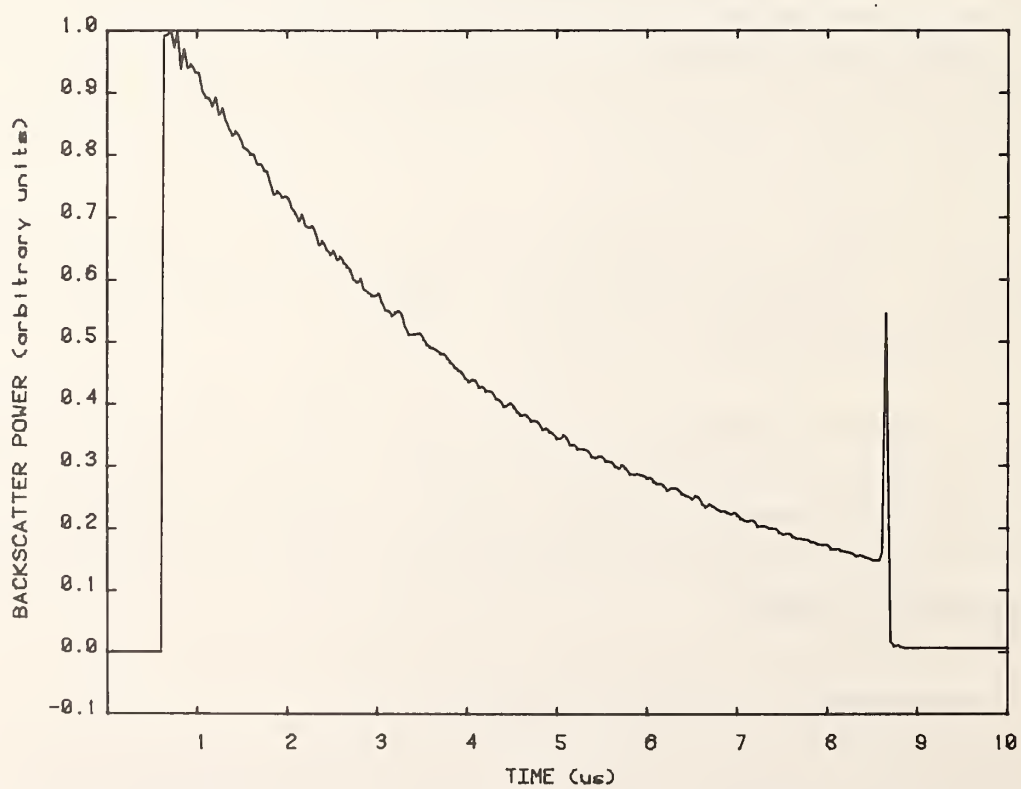

Figure 6-2. Center core concentric-core fiber, linear display. Launch conditions adjusted for maximum power transmission.

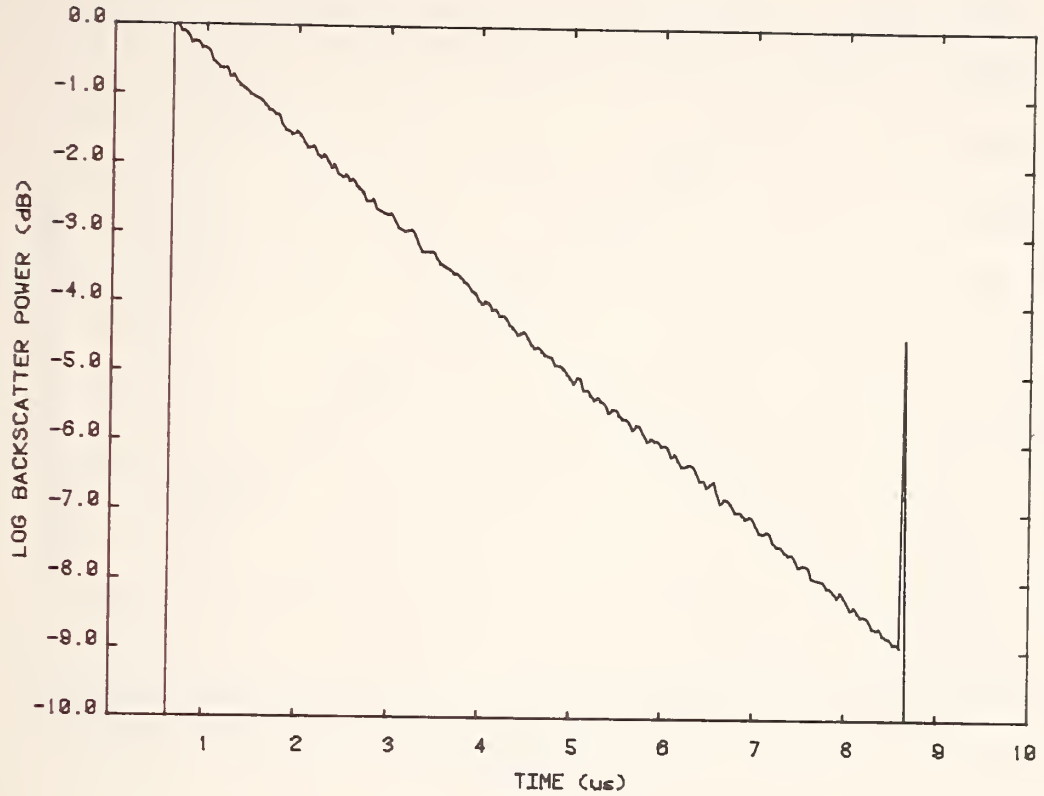

Figure 6-3. Center core concentric-core fiber, logarithmic display. Launch conditions adjusted for maximum backscatter signal.

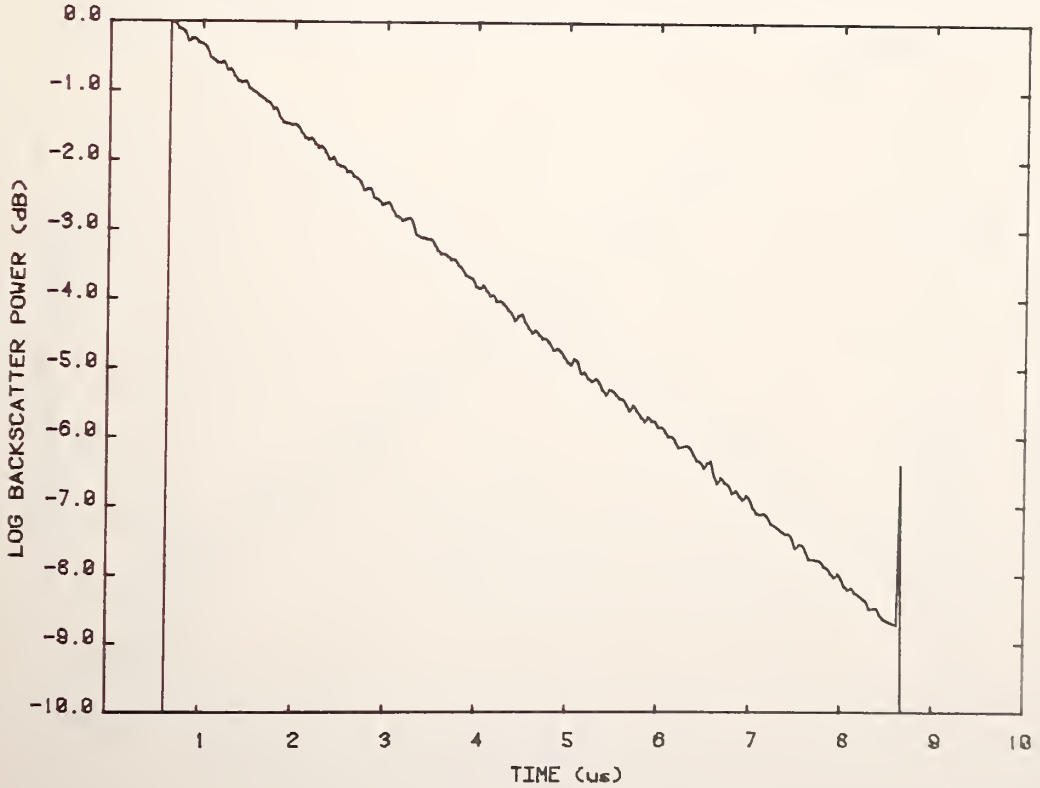

Figure 6-4. Center core concentric-core fiber, logarithmic display. Launch conditions adjusted for maximum power transmission.

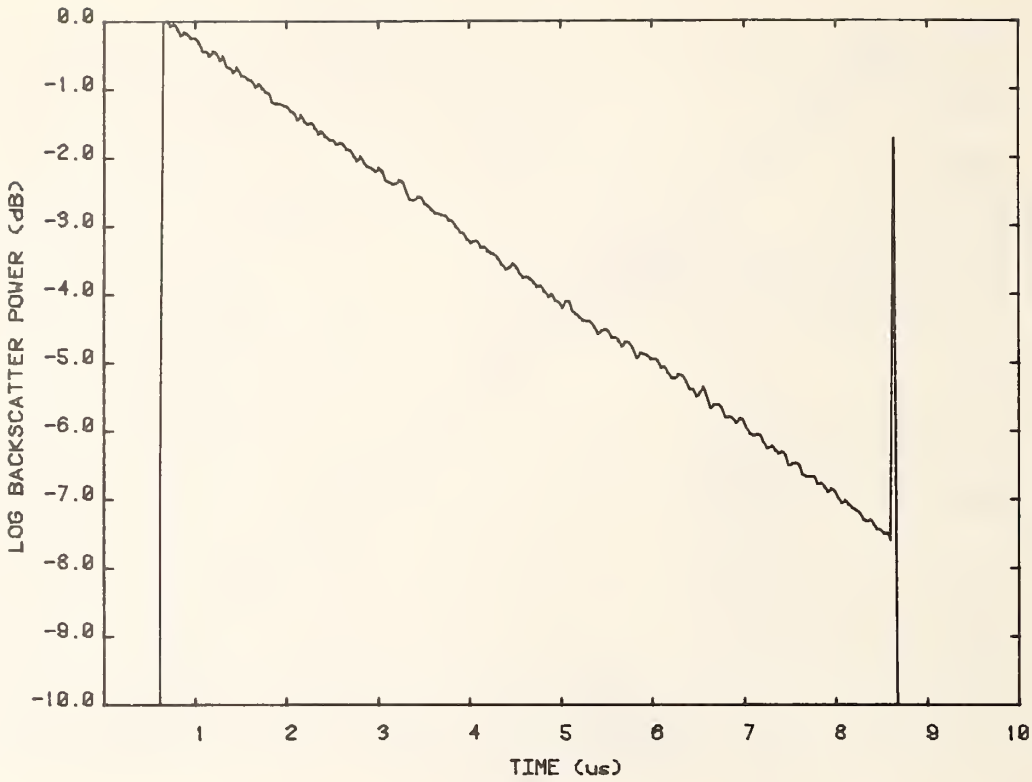

Figure 6-5. Center core concentric-core fiber, logarithmic display. Restricted launch conditions.

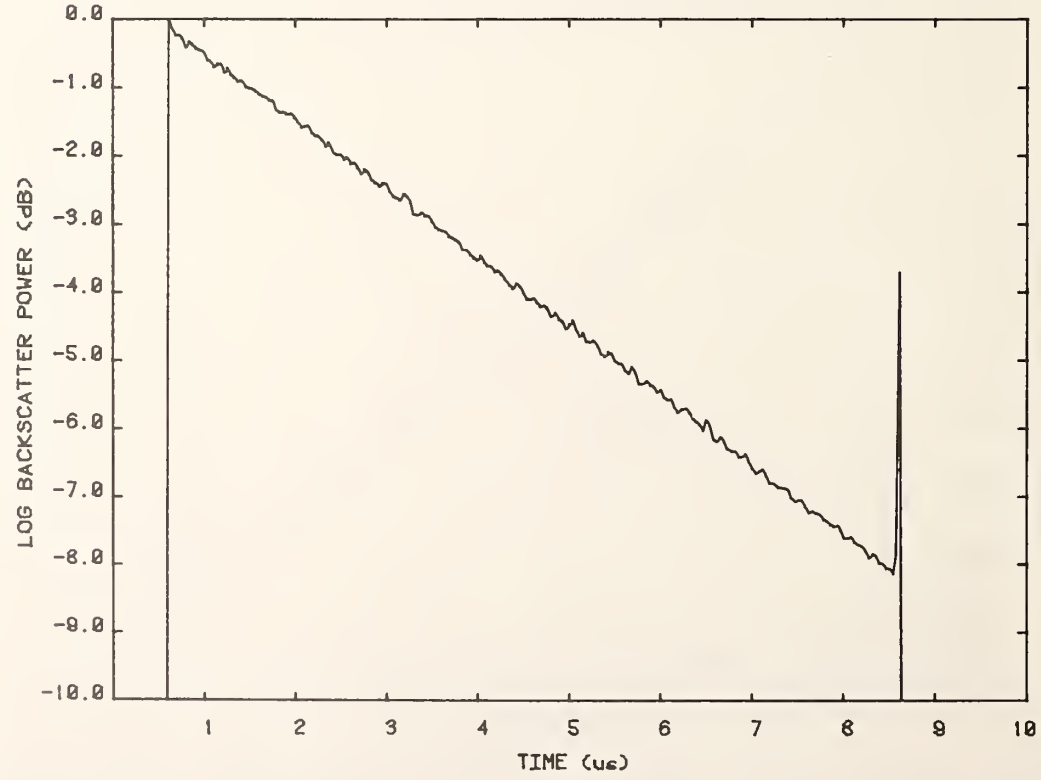

Figure 6-6. Outer core concentric-core fiber, logarithmic display. Launch conditions adjusted for maximum backscatter signal.

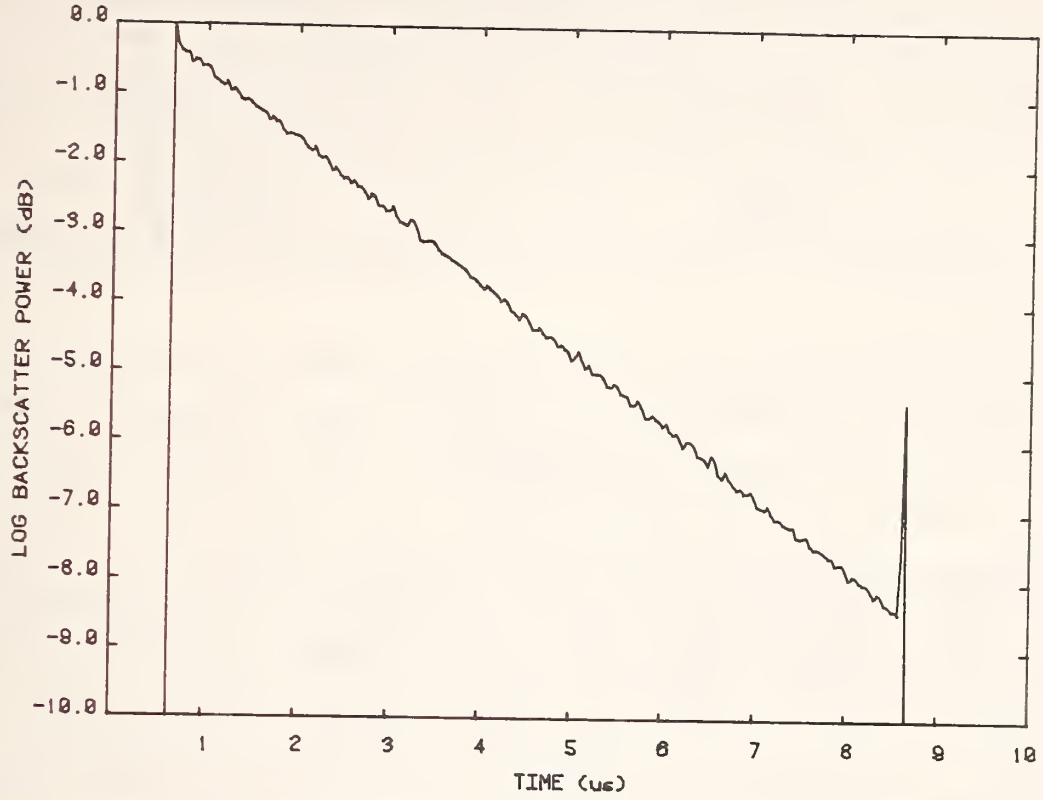

Figure 6-7. Outer core concentric-core fiber, logarithmic display. Launch conditions adjusted for maximum power transmission.

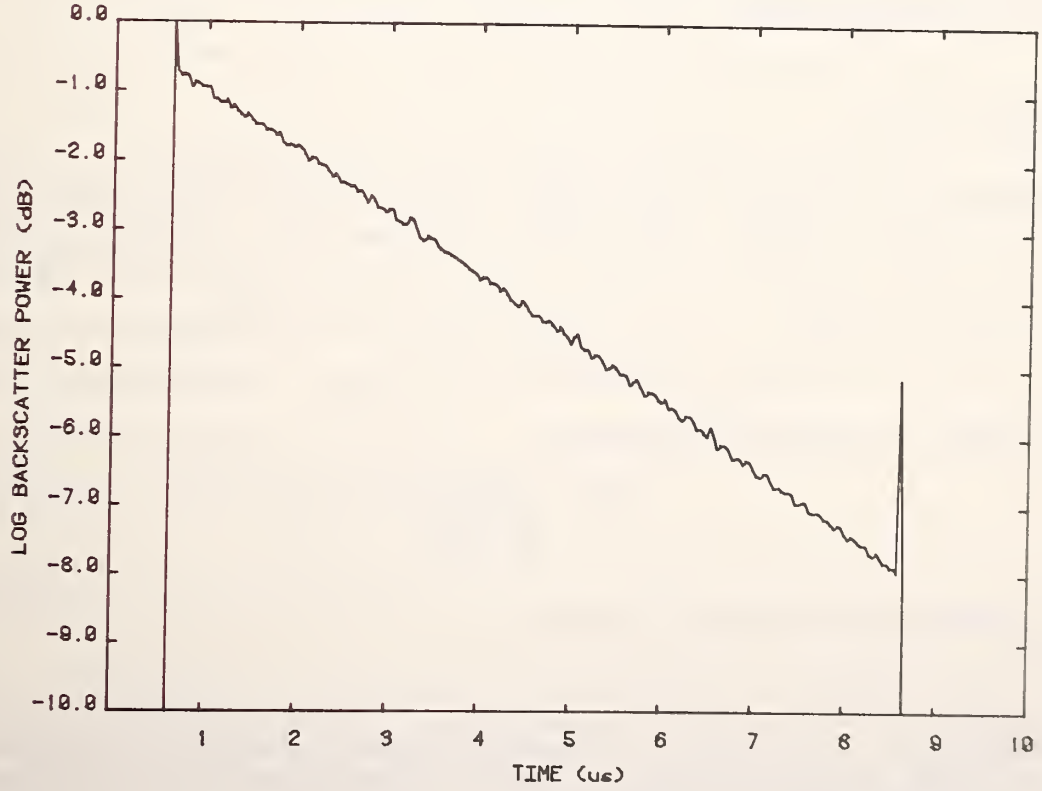

Figure 6-8. Outer core concentric-core fiber, logarithmic display. Restricted launch conditions.

wavelength of 850 nm using a GaAlAs laser diode emitting a probe pulse of about 20 ns duration. In the present application, aperture #1 was a pinhole of 25 μm diameter. Since the launch optics had a 1:1 magnification, the spot size at the front end of the fiber was also 25 μm. Aperture #2 shown in the figure had a diameter of 200 μm. The near-field radiation pattern emanating from the output end of the fiber was displayed on a silicon vidicon (not shown) in order to insure that the correct core was being excited. The logarithmic displays of the backscatter signals were calculated using a digital microcomputer.

Some representative backscatter signatures are shown in figures 6-2 to 6-8. These responses yield information on fiber length, overall attenuation, length dependence of loss, and diameter variations [17].[1] Three different launch conditions were used. In the first, the micropositioners on the launcher were adjusted so that a maximum backscatter amplitude registered on the oscilloscope at t = 0. In the second arrangement, the Fresnel reflection at the far end of the fiber was maximized. This approximated maximum power transmission through the fiber. The third launch condition was similar except that the input numerical aperture was decreased so that the backscatter signal was reduced by 6 dB. The fiber attenuation calculated from these backscatter responses is listed in table 2. It can be seen that the maximum scatter condition produces the highest attenuation values and the restricted launch the lowest. The variation in measured loss values points out the importance of specifying the exact conditions of excitation.

7. Capture Fraction

The magnitude of the backscatter signal from an optical fiber is proportional to that fiber's capture fraction. This quantity represents the relative amount of radiation scattered by the probe pulse which is subsequently trapped by the fiber and returned as guided radiation in the backward direction. The concept of a capture fraction is usually associated with Rayleigh scattering. The theoretical value for a step-index fiber is given by the relation

$$F = \frac{3}{8}\frac{(NA)^2}{n_1^2} \qquad (7\text{-}1)$$

and for a graded-index fiber the relation is

[1] Pulse broadening is also evident in figure 6-8 when the Fresnel reflections from the near and far ends of the fiber are compared. However, there is insufficient resolution in the present display to obtain accurate values of the pulse dispersion.

Table 4. Theoretical and measured capture fractions for the concentric core fiber.

Capture fraction	Center core
Theoretical	0.0034
Measured*	0.0066

*Uncertainties described in reference 16.

$$F = \frac{(NA)^2}{4n_1^2}. \qquad (7\text{-}2)$$

In both cases NA is the numerical aperture and n_1 the on-axis index of refraction [17]. The center core of the concentric-core fiber is approximately a step-index type, so that eq (7-1) would be expected to apply. However, this simple relationship will not be relevant to the outer core.

Experimental determinations of capture fractions can be made by a method proposed by Neumann [18] and described in detail elsewhere [17]. They are obtained from the measurement of the ratio of the power reflected from a cleaved end to the power backscattered from the fiber at that point. Capture fraction measurements have been made for the center core of the concentric-core fiber, and are listed in table 4. The uncertainties quoted in the table are calculated according to the error budget given in reference 17. It has been observed that the theoretical and measured values of F can differ by as much as a factor of three in some cases, so that the results given here are not surprising.

This work was supported by the Communications Systems Center, U.S. Army Communications R&D Command, Fort Monmouth, New Jersey 07703.

8. References

[1] Bender, A.; Salisbury, G.; Christian, R.; Steensma, P. Concentric-core optical fiber. Technical Digest of the Topical Meeting on Optical Fiber Communication; 1979 March 6-8; Washington, D.C. 102-104.

[2] Bender, R.; Concentric-core optical fiber subsystem, Technical Digest of the Conference on Lasers and Electrooptics; 1981 June 10-12; Washington, D.C. 116-117.

[3] Franzen, D.L.; G.W. Day; R.L. Gallawa; Standardizing test conditions for characterizing fibers; Laser Focus 17(8): 103-105;1981 August.
[4] Reitz, Paul R. Measuring optical waveguide attenuation: The LPS method. Optical Spectral 15(8):48-52; 1981 August.
[5] Holmes, G. T. and R. M. Hawk. Limited phase-space attenuation measurements of low-loss optical waveguides. Optics Letters 6(2):55-57; 1981 February.
[6] Cherin, A. H.; Gardner, W. Fiber measurement standards. Laser Focus 16(8):60-65; 1980 August.
[7] Kaiser, P. Low measurements of graded-index fibers: accuracy vs. convenience. Technical Digest, Symposium on Optical Fiber Measurements, Nat. Bur. Stand. (U.S.) Spec. Publ. 597; 1980.
[8] Cherin, A. H.; E. D. Head. A fiber concatenation experiment using a standardized loss measurement method. Technical Digest, Symposium on Optical Fiber Measurements, Nat. Bur. Stand. (U.S.) Spec. Publ. 597; 1980.
[9] Franzen, D. L.; Day, G. W.; Danielson, B. L.; Chamberlain, G. E.; Kim, E. M. Interlaboratory measurement comparison to determine the attenuation and bandwidth of graded-index optical fibers. Appl. Opt. 20(14):2412-2419; 1981 July 15.
[10] Inada, K. A new graphical method relating to optical fiber attenuation. Opt. Commun. 19(3):437-439; 1976 December.
[11] Kim, E. M.; Franzen, D. L. Measurement of far-field and near-field radiation patterns from optical fibers. Nat. Bur. Stand. (U.S.) Tech. Note 1032; 1981 February. 48 p.
[12] Franzen, D. L.; Day, G. W. Measurement of optical fiber bandwidth in the time domain. Nat. Bur. Stand. (U.S) Tech. Note 1019; 1980 February. 72 p.
[13] White, K. I. Practical application of the refracted near-field technique for the measurement of optical fiber refractive index profiles. Opt. Quantum Electron. 11:185-188; 1979.
[14] Stewart, W. J. A new technique for measuring the refractive index profiles of graded optical fibers. Technical Digest, IOOC; 1977 July 18-20; Tokyo, Japan. 1977 July. 395-398.
[15] Young, M. Refracted-ray scanning (refracted near-field scanning) for measuring index profiles of optical fibers. Nat. Bur. Stand. (U.S.) Tech. Note 1038; 1981.
[16] Young, M. Optical fiber index profiles by the refracted ray method (refracted near-field scanning). Appl. Opt. 20(19):3415-3422; 1980 October 1.
[17] Danielson, B. L. Backscatter measurements on optical fibers. Nat. Bur. Stand. (U.S.) Tech. Note 1034; 1981 February. 52 p.
[18] Neumann, E. G. Analysis of the backscattering method for testing optical fiber cables. AEU, Electron. and Commun. 34(4):157-160; 1980.

NBS-114A (REV. 2-8C)

U.S. DEPT. OF COMM. BIBLIOGRAPHIC DATA SHEET (See instructions)	1. PUBLICATION OR REPORT NO. NBSIR 82-1661	2. Performing Organ. Report No.	3. Publication Date April 1982

4. TITLE AND SUBTITLE

Characterization of a Concentric-Core Fiber

5. AUTHOR(S)

B. L. Danielson, D. L. Franzen, R. L. Gallawa, E. M. Kim, M. Young

6. PERFORMING ORGANIZATION (If joint or other than NBS, see instructions)

NATIONAL BUREAU OF STANDARDS
DEPARTMENT OF COMMERCE
WASHINGTON, D.C. 20234

7. Contract/Grant No.

8. Type of Report & Period Covered
Final
10/1/80-10/1/81

9. SPONSORING ORGANIZATION NAME AND COMPLETE ADDRESS (Street, City, State, ZIP)

Communications Systems Center
U.S. Army Communications R&D Command
Fort Monmouth, New Jersey 07703

10. SUPPLEMENTARY NOTES

☐ Document describes a computer program; SF-185, FIPS Software Summary, is attached.

11. ABSTRACT (A 200-word or less factual summary of most significant information. If document includes a significant bibliography or literature survey, mention it here)

Several optical properties of a concentric-core fiber are examined. These include attenuation, radiation patterns, pulse broadening, index profile, backscatter signatures, and capture fraction. Experimental techniques are briefly described and the significance of the measured parameters is discussed.

12. KEY WORDS (Six to twelve entries; alphabetical order; capitalize only proper names; and separate key words by semicolons)

Attenuation; backscatter; backscatter signatures; capture fraction; concentric-core fiber; fiber optics; index profile; optical time domain reflectometer; OTDR; pulse broadening; radiation patterns.

13. AVAILABILITY

☒ Unlimited
☐ For Official Distribution. Do Not Release to NTIS
☐ Order From Superintendent of Documents, U.S. Government Printing Office, Washington, D.C. 20402.
☒ Order From National Technical Information Service (NTIS), Springfield, VA. 22161

14. NO. OF PRINTED PAGES
28

15. Price
$7.50

USCOMM-DC 6043-P80

☆ U.S. GOVERNMENT PRINTING OFFICE: 1982—578-894 214 REGION No. 8